# Nucleosome structure in diverse ionic environments.

Igor Nazarov[1]*, Iana Chekliarova[1], Georgy Rychkov[2,3], Andrey V. Ilatovskiy[3,4], Colyn Crane-Robinson[5] and Alexey Tomilin[1]

[1] Institute of Cytology, RAS, Tikhoretski ave. 4, Saint-Petersburg, RF, 194064
[2] Institute of Physics, Nanotechnology and Telecommunications, NRU Peter the Great St.Petersburg Polytechnic University, Polytechnicheskaya 29, Saint-Petersburg, RF, 195251
[3] Department of Molecular and Radiation Biophysics, National Research Centre "Kurchatov Institute" B.P. Konstantinov Petersburg Nuclear Physics Institute, Orlova Roscha, Gatchina, Leningrad District, RF, 188300
[4] Skaggs School of Pharmacy and Pharmaceutical Sciences, University of California, San Diego, 9500 Gilman Dr, La Jolla, CA 92093, USA
[5] Biophysics Laboratories, St. Michael's Building, University of Portsmouth, Portsmouth, PO1 2DT, UK

[*] To whom correspondence should be addressed, e-mail: i.nazarov@incras.ru

Keywords: Nucleosomes, AFM, 30 nm fibre, superhelical turns

Running Title: Nucleosome structure

**ABSTRACT**

Atomic force microscopy (AFM) was used to study mononucleosomes reconstituted from a DNA duplex of 353 bp containing the strong 601 octamer positioning sequence, together with recombinant human core histone octamers. Three parameters were measured: 1) the length of DNA wrapped around the core histones; 2) the number of superhelical turns, calculated from the total angle through which the DNA is bent, and 3) the volume of the DNA-histone core. This approach allowed us to define in detail the structural diversity of nucleosomes caused by disassembly of the octasome to form subnucleosomal structures containing hexasomes, tetrasomes and disomes. At low ionic strength (TE buffer) and in the presence of physiological concentrations of monovalent cations, the majority of the particles were subnucleosomal, but physiological concentrations of bivalent cations resulted in about half of the nucleosomes being canonical octasomes in which the exiting DNA duplexes cross orthogonally. The dominance of this last species explains why bivalent but not monovalent cations can induce the initial step towards compaction and convergence of neighboring nucleosomes in nucleosomal arrays to form the chromatin fiber in the absence of linker histone. The observed nucleosome structural diversity may reflect the functional plasticity of nucleosomes under physiological conditions.

## 1. INTRODUCTION

Eukaryotic genomic DNA exists in a highly compact and organized form called chromatin. For many years it was thought that the chromatin in the cell nucleus exists mainly in the form of 30 nm fibrils composed of regularly repeated core particles connected by a certain length linker DNA and linker histones. Much evidence for such fibers of several structural types has been obtained *in* vitro [1-3], but the evidence for 30-nm fibers *in vivo* is not overwhelming. The nucleosome fiber *in vivo* appears to be dynamic, existing as an irregularly folded structure subject to Brownian motion and ongoing processing [4-7].

The mono-nucleosome as the basic structural unit of chromatin [8] is sufficiently stable to maintain structures of higher order but it must also ensure the accessibility of the information encoded in the DNA, i.e. it behaves as a dynamic structure that can reversibly change its conformation and composition. Data showing that the histone octamer can stably package from about 100 to 170 bp of DNA has been presented [9-13]. Moreover, more recent findings lead to the conclusion that the nucleosome must be considered as a family of particles, which differ not only in the amount of DNA wrapped around the core histone proteins but also in the composition of the internal histone core: octasomes, hexasomes, tetrasomes, "split" half-nucleosomes, hemisomes, lexosomes, [14-20]. An integral feature of chromatin and nucleosomes is their high sensitivity to changes in the environment. Studies carried out under even slightly differing conditions are difficult to compare and the ionic environment affects both internucleosomal and intranucleosomal interactions [21].

Here we investigate the effect of ionic conditions on mononucleosome conformation and its structural variants using an analysis of multiple atomic force microscopy (AFM) images to define the conformation of the entering and exiting DNA strands from a positioned histone core, all in the absence of linker histone. This is not a totally artificial situation because it is well established that in the presence of $Mg^{2+}$ ions, despite the absence of linker histone, the 30-nm fiber is readily formed [22, 23].

Single nucleosome analysis has allowed us to define the structural diversity of nucleosomes as a consequence of the unwrapping of DNA and partial histone octamer dissociation. Under conditions of low nucleosome concentration the structural distribution exhibited four distinct major subpopulations of nucleosomes, verified to be disomes, tetrasomes, hexasomes and octasomes. Low ionic strength and the presence of monovalent cations favored disassembled species, whilst bivalent cations shifted the distribution to octasomes, in particular a form in which the DNA duplexes exit the nucleosome orthogonally.

## 2. MATERIALS and METHODS

### 2.1. DNA, histones and nucleosome reconstitution

A DNA fragment, 353 bp in length, containing the strong 601 nucleosome positioning sequence was amplified by the polymerase chain reaction using plasmid pGem-3Z-601 (derived from Widom's laboratory) as a template [24]. The primers were designed such that the dyad symmetry nucleotide (S0 site) was located asymmetrically: 200 bp from one end, correspondingly 152 bp from the other end. Core histone octamer refolding and nucleosome reconstitution were performed according to protocols from the Luger laboratory [25] using full-length human recombinant histones purchased from New England Biolabs. In brief, H2A, H2B, H3 and H4 histones were transferred to unfolding buffer (6M guanidinium hydrochloride, 20 mM Tris-HCl, pH 7.5, 5 mM DTT), mixed in equimolar ratios at a final protein concentration of ~1 mg/ml. The histone mixture was then stepwise dialyzed using Slide-A-Lyzer 7K dialysis cassettes (Pierce) against refolding buffer (2M NaCl, 10 mM Tris-HCl, pH 7.5, 1 mM EDTA, 5 mM 2-mercaptoethanol) at $4^0$ C. After concentration to 5 mg/ml, the products were loaded onto a Superdex 200 PG column (4 mm x 30 mm) equilibrated with refolding buffer. Chromatography was performed at $4^0$ C, the flow rate was 0.04 ml/min, fraction volumes 75 μl. Fractions containing histone octamers were pooled and kept on ice at ~ 2 mg/ml before use. For nucleosome reconstitutions, a micro-scale stepwise dilution protocol was used [25]. A molar ratio of 1/1 for DNA to octamers with a Slide-A-Lyzer Mini Dialysis Unit MWCO 3500 (Pierce) was used in overnight dialysis against buffer containing 0.2 M NaCl followed by a 2 hr dialysis against TE buffer. After determining concentrations the samples were kept on ice at a DNA concentration of ~75 μg/ml until used.

### 2.2. Surface preparation, sample preparation and AFM

Nucleosomes were immobilized on the surface of aminopropyl-triethoxysilatrane APS-treated mica [26]. The nucleosome samples were diluted to a final DNA concentration of 0.5 μg/ml (~2 nM) with 10 mM Tris-HCl buffer, pH 7.5, together with 1 mM EDTA, or NaCl, or $MgCl_2$ at different concentrations and then incubated for 5 min at room temperature (RT). 5 μl droplets were deposited onto the mica surface, left for 3 min at RT and the surfaces then rinsed with Milli-Q Ultrapure water, dried in an argon flow and kept under vacuum. The samples were scanned in tapping mode in air at RT using a Nanoscope III system (Veeco, Santa Barbara, CA, USA) using silicon probes with a spring constant of 42 N/m and a resonant frequency of 320 kHz. The scanning rate was 1.7 Hz over scan areas of 1 μm and images were captured in a 512 x 512 pixel format and flattened before analyses. Measurements of contour length, angle and cross-section analysis were performed using Femtoscan software (Advanced Technologies Center, Moscow, Russia).

### 2.3. Nucleosome image analysis

AFM images of nucleosomes were used to analyze wrapped DNA length (Lw), the volume of the DNA-protein core (V), and the number of DNA superhelical turns around the histone core (Nt). A typical field is shown in Figure S1. The length of each arm was measured from the end at half DNA height up to the perpendicular line crossing the nucleosome core through its centroid (see Fig. 1). Wrapped DNA length, Lw, was calculated from the equation: Lw = Lt – L1 –L2, where Lt is the template DNA length and L1, L2 the measured DNA arm lengths.

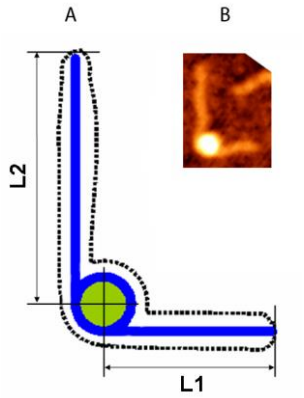


Fig. 1. **A.** Schematic representation of DNA arm length measurement. The green circle is the histone core. Blue solid lines represent the real DNA contour. Black dashed lines represent the observed nucleosome contour in AFM images. L1, L2 are DNA arm lengths. The length of the each arm was measured from its end (at half of DNA height) up to the perpendicular line crossing the nucleosome core through its centroid. **B** is an AFM image corresponding to the nucleosome drawn in A.

The volume of the nucleosome core, i.e. excluding the unwrapped DNA 'tails', was calculated by treating the particle as a segment of a sphere [27]: $V = \pi h/6 \times (3r^2 + h^2)$, where h is the height and r the radius.

Fig. 2 shows the approach for calculating ∠r, the angle through which the DNA is bent and for determining the number of DNA turns (Nt) from the angle measured between the exiting DNA arms (∠m). Due to the fact that the ∠m value is cyclically repeated for variants of partially assembled and folded nucleosomes, the images were sorted by type using the Lw value and an appropriate formula applied for ∠r calculation:

Type 1: ∠r = 180° – ∠m, if Lw < 41.7 bp,

Type 2: ∠r = 180° + ∠m, if 41.7 bp ≤ Lw < 83.4 bp,

Type 3: ∠r = 540° – ∠m, if 83.4 bp ≤ Lw < 125.1 bp,

Type 4: ∠r = 540° + ∠m, if 125.1 bp ≤ Lw

The number of DNA turns (Nt) was calculated from the equation: Nt = ∠r /360°

**Nucleosome images**

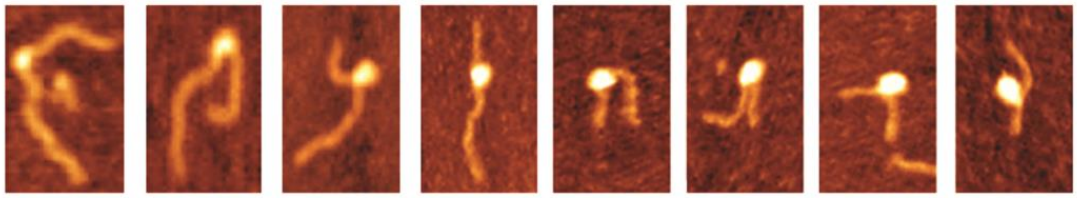

**Nucleosome models**

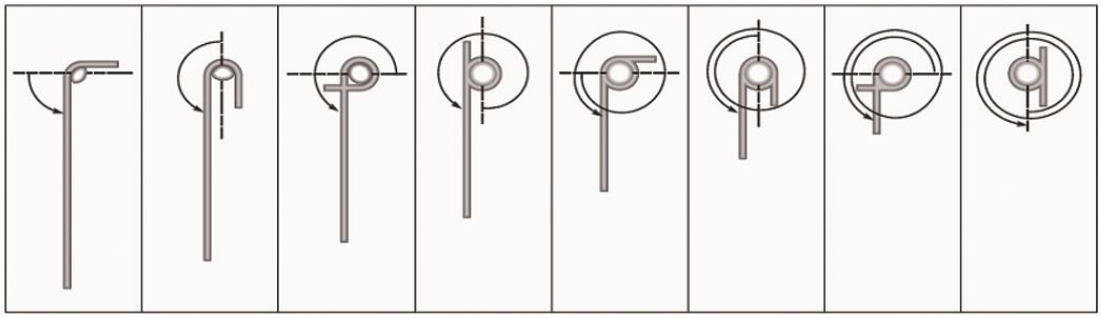

| | | | | | | | | |
|---|---|---|---|---|---|---|---|---|
| Measured angle, ∠m | 90° | 0 ° | 90° | 180° | 90 ° | 0° | 90° | 180° |
| Wrapped DNA length, Lw | 20.9 | 41.7 | 62.6 | 83.4 | 104.3 | 125.1 | 146 | 166.8 |
| Type / criterion | **1** Lw < 41.7 | | **2** 41.7 < Lw < 83.4 | | **3** 83.4 < Lw <125.1 | | **4** 125,1 < Lw | |
| Formula for ∠r | ∠r = 180° - ∠m | | ∠r = 180° + ∠m | | ∠r = 540° - ∠m | | ∠r = 540° + ∠m | |
| Angle of DNA bending, ∠r | 90° | 180° | 270° | 360° | 450° | 540° | 630° | 720° |
| Number of turns, Nt | 0.25 | 0.5 | 0.75 | 1.00 | 1.25 | 1.50 | 1.75 | 2.00 |

Fig. 2. Nucleosome variants and their characteristics obtained from analysis of AFM images. The top row gives examples of nucleosome images corresponding to the models in the second row and their characteristics arranged in the table columns below. Curved arrows in the models indicate the total DNA bending angle (∠r) relative to unbent DNA template. Columns give corresponding values of measured angle (∠m), measured wrapped DNA length (Lw), the calculated bending angles ∠r, the calculated number of superhelical turns (Nt). Rows 3 and 4 give information for type-dependent calculations.

## 3. RESULTS

Nucleosomes were reconstituted using a 353-bp duplex containing the 601 positioning sequence together with recombinant core histone octamers, i.e. lacking post-translational modifications. The homogeneity of the nucleosome samples was confirmed by electrophoresis (Fig. 3). They were spread on mica films and

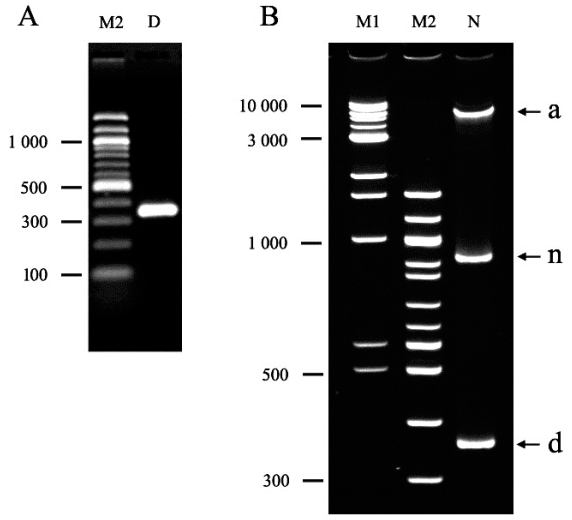


Fig. 3: **A:** Electrophoresis of template DNA: ethidium bromide stained 1.5 % agarose gel electrophoresis in 0.5 x TBE of the 353-bp DNA fragment (track D) containing the nucleosome-positioning sequence.
**B:** ethidium bromide stained 6% polyacrylamide gel electrophoresis in 0.5 x TBE of a reconstituted nucleosome sample. The labels **d**, **n**, and **a** correspond to free DNA, the mononucleosome and a higher-molecular weight structure [25], respectively. M1 and M2 are molecular weight markers.

multiple images of both naked DNA and nucleosomes collected and analyzed. To estimate the experimental variation, the lengths of 316 free DNA molecules were measured, showing a Gaussian distribution centered at 120.8 ± 4.0 nm (mean ± SD); this corresponds to B-form DNA having a 10-bp repeat of 3.4 nm (see Figure S2). For nucleosomes, three measurements were made of a total of 803 images: 1) the lengths of the DNA arms (see Fig. 1 for an explanation of this measurement), 2) the angle between the two exiting duplexes and 3) the volume of the histone-DNA core. The lengths of the DNA arms and the angle between the two exiting duplexes were used to calculate the length of the DNA wrapped around the histone core (Lw) and the number of superhelical turns (Nt) – see Materials and Methods. These two quantities are, of course, related in that Lw/Nt represents the length of one superhelical turn. The data fit to a Gaussian distribution about a value of 83.4 ± 6.2 bp (Mean ± SD, n = 172), which is taken as the wrapped length in one superhelical turn (see Figure S3).

The approach used for the calculations is shown in (Fig. 2). Errors were estimated for Lw, Nt and V of nucleosome samples obtained from 5 independent measurements of 3 different images of the 3 same objects, resulting in 15 values of each parameter per object. All 9 data sets (for 3 parameters of 3 objects) were found to be normally distributed using the Shapiro-Wilk W-test for normality and the relative errors were calculated as the ratios of the half-widths of 95% confidence intervals to the object mean value. The relative errors for each parameter were: 4%, 12% and 20% for Nt, Lw and V, respectively.

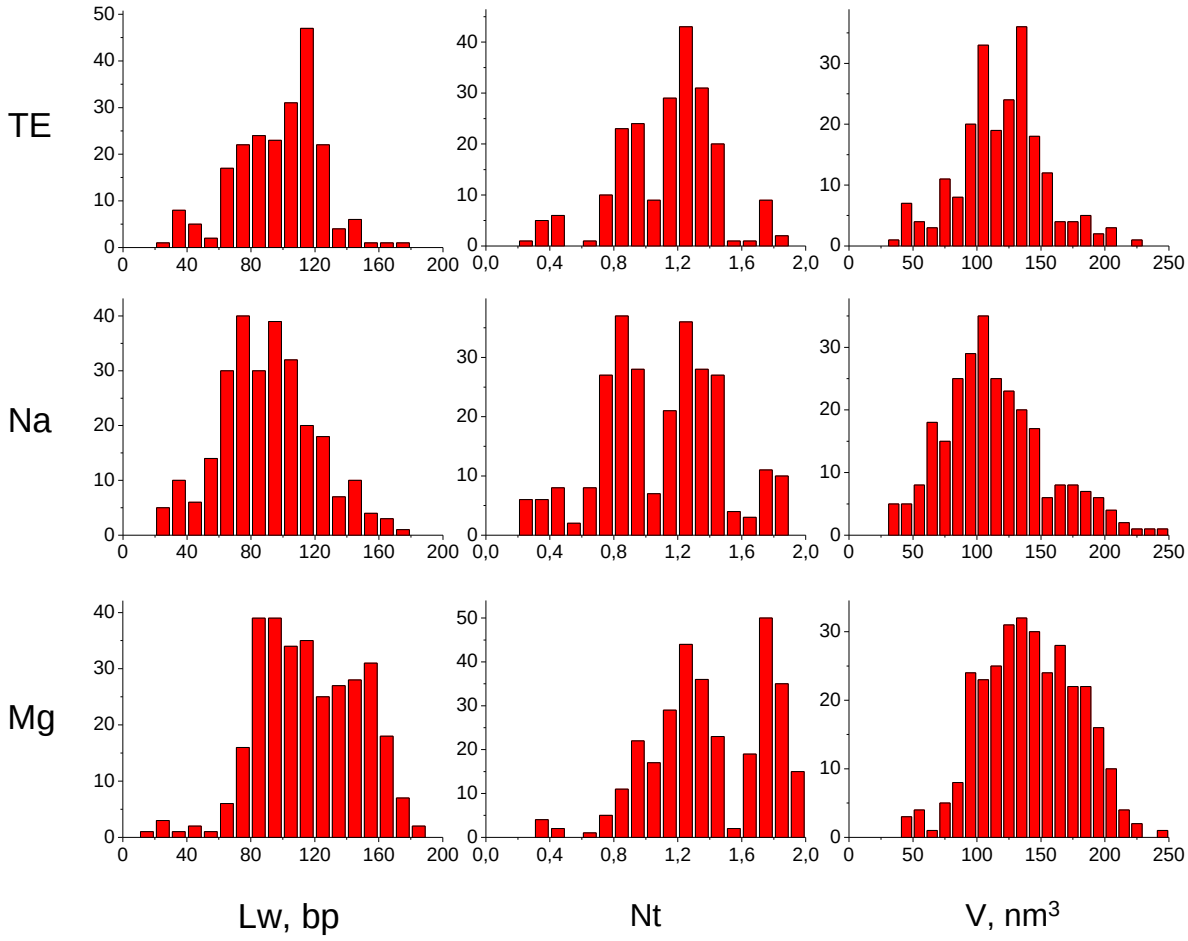


Fig. 4. Value distributions of wrapped nucleosome DNA length (Lw), the number of DNA superhelical turns (Nt), and the nucleosome volume in TE buffer (n = 215); in 10 mM Tris-HCl, pH 7,8 + 140 mM NaCl (n = 270) and in 10 mM Tris-HCl, pH 7,8 + 4 mM $MgCl_2$ (n = 318).

Fig. 4 presents distributions of Lw, Nt and V. The three distributions for Nt clearly show four separate peaks centered at about 0.35, 0.85, 1.3 and 1.8 superhelical turns, though such peaks can only partially be discerned in the Lw and V distributions, a difference clearly stemming from the greater accuracy of the Nt measurements. Comparing the distributions in different ionic environments shows that whereas the addition of 140 mM NaCl to the TE buffer results in only a slight redistribution of particle species, the presence of 4 mM $Mg^{2+}$ drives many nucleosomes to increased values of Lw, Nt and V.

In order to better define particle distributions, Fig. 5 presents 2D scatter plots of wrapped nucleosome DNA length (Lw) against the number of DNA superhelical turns (Nt). As expected, a good linear correlation between these two, linked, parameters is seen, despite the inevitable observational scatter. The existence of four sub-groups of particles is more apparent in Fig. 5 than in Fig. 4 and to emphasize this more clearly, the data are also plotted as density profiles on the right hand side of Fig. 5. This shows that the main peaks are centered at: 1) Nt = 1.75, Lw = 147 bp; 2) Nt = 1.25, Lw = 106 bp; 3) Nt = 0.85, Lw = 72 bp; 4) Nt = 0.40, Lw = 39 bp.

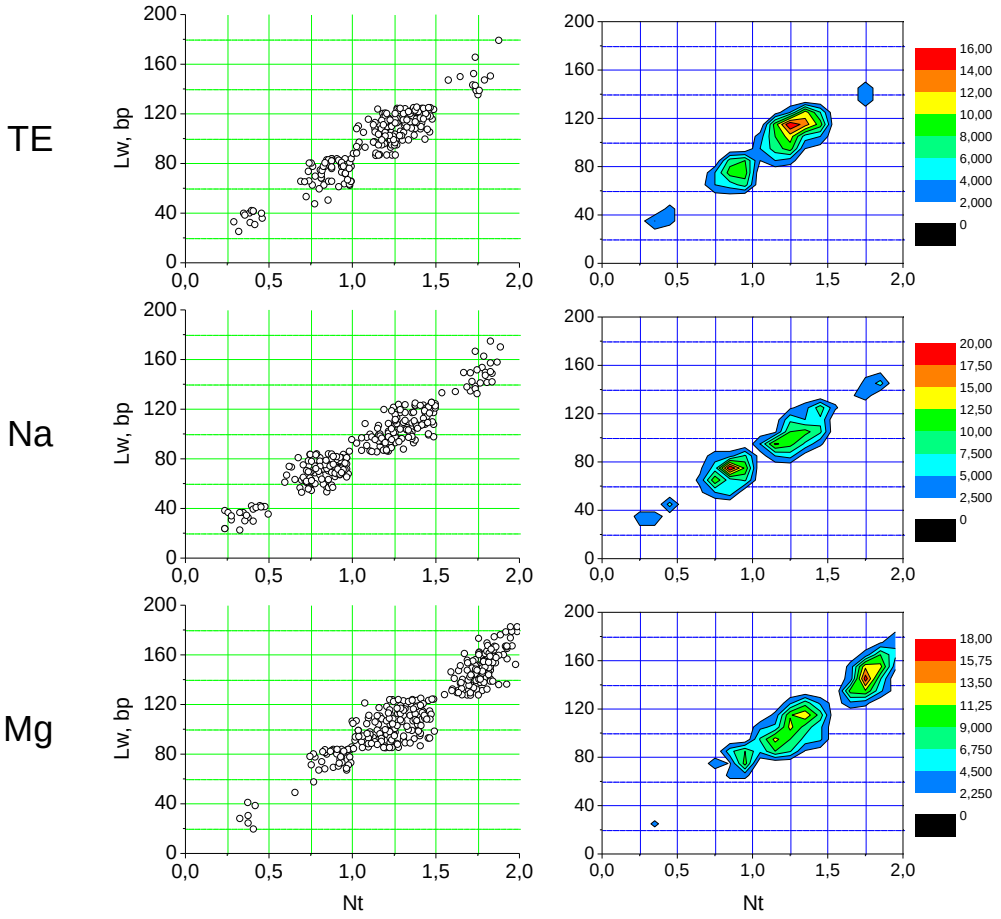


Fig. 5. Plots of wrapped nucleosome DNA length (Lw) against the number of DNA superhelical turns (Nt) in TE buffer (n = 215); in 10 mM Tris-HCl, pH 7,8 + 140 mM NaCl (n = 270) and in 10 mM Tris-HCl, pH 7,8 + 4 mM $MgCl_2$ (n = 318). Left hand panels are scatter plots, right hand panels are dot density plots.

To determine what these four populations represent, i.e. to what sub-nucleosomal species they should be assigned, Nt values were plotted against the volumes of the particles – two quite independent parameters – and this is shown in Fig. 6 - that also displays density plots in the right hand panels.

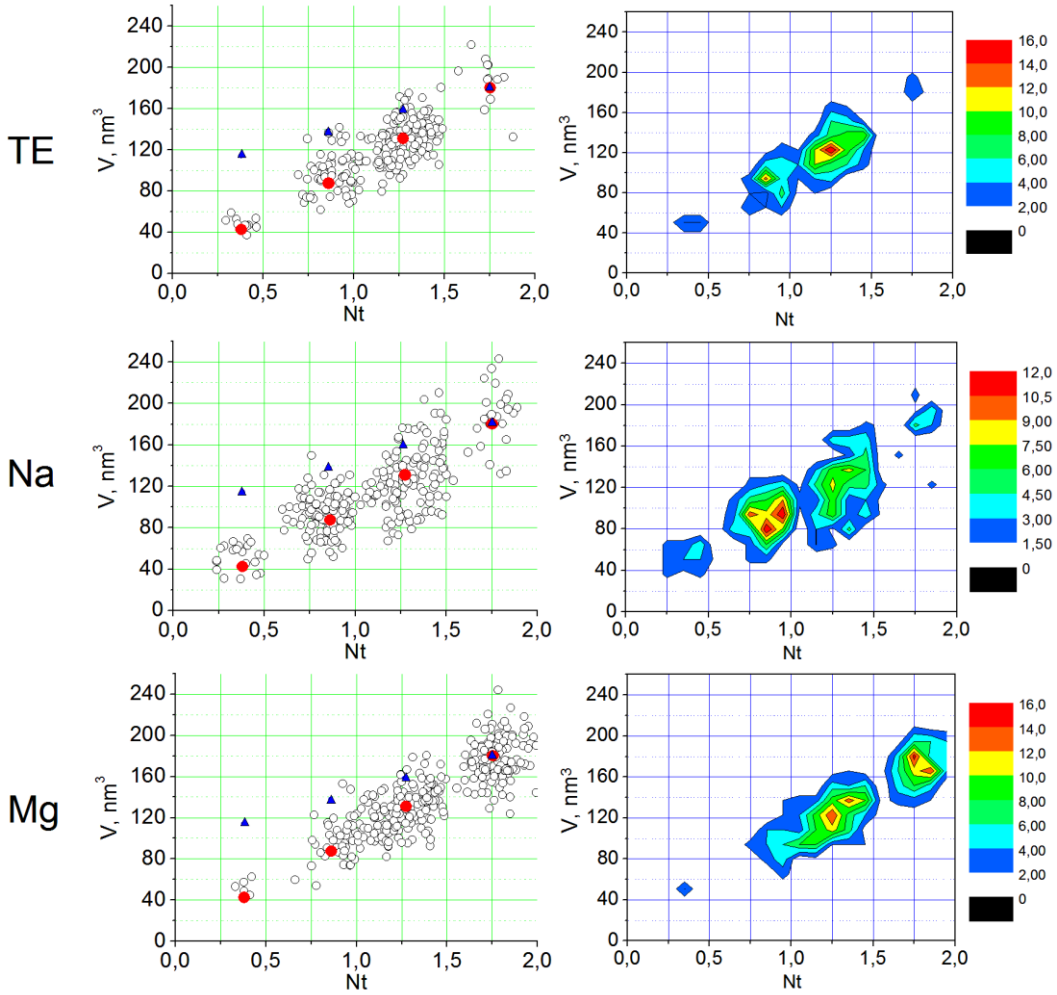


Fig. 6. Plots of nucleosome volume (V) against the number of DNA superhelical turns (Nt) in TE buffer (n = 215); in 10 mM Tris-HCl, pH 7,8 + 140 mM NaCl (n = 270) and in 10 mM Tris-HCl, pH 7,8 + 4 mM $MgCl_2$ (n = 318). Left hand panels are scatter plots and the red dots represent the relative volumes, V, of octasome, hexasome, tetrasome and disome, as given in Table 1. The blue triangles represent the predicted relative volumes of particles having the same Nt values but retaining the full complement of octameric core histones. The right hand panels are dot density plots, as in Fig. 5.

There is inevitably a greater scatter in Fig. 6 than in Fig. 5 in consequence of the greater error in the volume measurements but the four principal components remain clearly visible. The particles with lower Nt (Lw) values, i.e. those from which significant lengths of DNA has unwrapped, are likely to represent species that have also lost histones – but is this hypothesis consistent with their measured volumes? The expected volumes, V, of three sub-nucleosomal species, (hexasome, tetrasome and disome), were predicted using the Nt = 1.75 octasome particle (mass 204 kDa, measured volume 180 $nm^3$) as calibrant, by calculating their volume fractions, $V_f$, from their masses, i.e. assuming uniform density. Bearing in mind that only the volume of the central particle is measured, (i.e. excluding the extended DNA arms), their masses represent the sum of the histones and that of the remaining wrapped DNA, given by the mean values of Lw observed for the given subpopulation, (see Table 1).

Table 1. Fractional volumes ($V_f$) of subnucleosomal particles calculated from molecular weights and normalised relative to an octasome volume of 1, experimentally measured as 180 $nm^3$.
* Mean values of Lw observed for the given subpopulation.

| Particle | Composition | Mw, kDa | $V_f$, fraction | V, $nm^3$ |
|---|---|---|---|---|
| Dimer | H2A/H2B | 27,8 | 0,14 | 24,5 |
| Tetramer | 2(H3/H4) | 53,0 | 0,26 | 46,8 |
| Hexamer | 2(H3/H4) H2A/H2B | 80,8 | 0,40 | 71,3 |
| Octamer | 2(H3/H4) 2(H2A/H2B) | 108,6 | 0,53 | 95,8 |
| DNA | 147 bp | 95,4 | 0,47 | 84,2 |
| **Octasome** | **Octamer + 147 bp DNA** | **204,0** | **1,00** | **180** |
| Hexasome | Hexamer + 106 bp* DNA | 149,6 | 0,73 | 131,9 |
| Tetrasome | Tetramer + 72 bp* DNA | 99,7 | 0,49 | 88,0 |
| Disome | H3/H4 Dimer + 39 bp* DNA | 51,8 | 0,25 | 45,7 |

Fig. 6 plots these (relative) volumes against their Nt values for the 4 principal components as red dots and these clearly coincide with the four centers of local particle density, strongly implying that they represent subnucleosomal species containing dimers, tetramers, hexamers and octamers of histones.

Another possibility to be considered, and by way of control, is that partial unwrapping of DNA in particles with lower Nt (Lw) values is *not* accompanied by histone loss. In that case, the reduced volume is a consequence only of DNA loss. Calculating the predicted volumes by the above method inevitably yields volumes greater than for the histone-depleted particles and these are plotted as blue triangles in Fig. 6: clearly, they do not coincide with the points of high particle density. We conclude that the species centered at Nt = 1.25, 0.85 and 0.40 truly represent partially unwrapped and depleted particles containing hexamers, tetramers and dimers of core histones. The specific assignment of partially assembled nucleosome populations was initially based on matching Lw and V parameters obtained from atomistic structures of sub-nucleosome particles [28,29].

From Figs. 5 and 6 it can be seen that the local centers of subnucleosomal particle distributions do not significantly change position over the three tested ionic conditions, as expected for such defined species, but their relative amounts change considerably. Addition of 140 mM NaCl to Tris buffer has only a slight effect on the hexamer to tetramer ratio, leaving the amounts of dimer and octamer species quite low. However, addition of 4 mM $Mg^{2+}$ leads to almost complete depletion of the disome and a large increase in the octasome population: the hexasome population also increases at the expense of the tetrasome.

In order to better monitor the ionic strength dependence of the distribution of subnucleosomal species the amount of NaCl added to Tris buffer was varied, as was the concentration of $Mg^{2+}$. The results are shown in Fig. 7 that plots the frequency of octasome occurrence against the ionic conditions.

It is seen that whereas addition of $Na^{+}$ has very little effect on octasome formation, the divalent cation $Mg^{2+}$ has a striking effect, peaking at about 4 mM. The drop-off at even higher concentrations of $Mg^{2+}$ probably results from release of histones, i.e. reversion to hexamer etc.

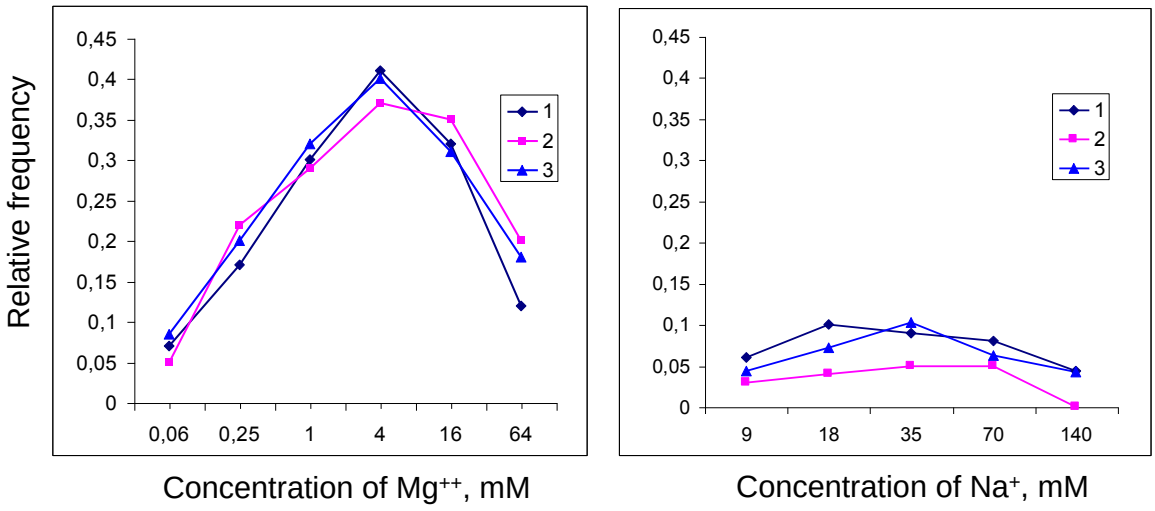


Fig. 7. Relative frequencies of octasomes in 10 mM Tris-HCl, pH 7,8 with different concentrations of $MgCl_2$ (left) or NaCl (right). 1, 2, 3 – the data of three independent experiments, each of which represents the results of a separate nucleosome reconstitution and sample preparation. Each point represents the analysis of more than a hundred individual nucleosomes.

The distribution of nucleosomal species was also tested in the presence of other monovalent and divalent cations: in 1×TBE buffer and in 10 mM Tris-HCl, pH 7.8 + 140 mM KCl, dissociation was similar to that in TE or NaCl buffer, while 4 mM $Ca^{++}$ had a somewhat stronger stabilizing effect as compared to 4 mM $Mg^{++}$ (data not shown).

## 4. DISCUSSION

It is well known that the nucleosomal particle is dynamic and can dissociate at low concentrations [30-32]: the functional importance of H2A/H2B dimer loss being first noted in 1983 [33]. AFM sample preparation requires dilution of nucleosomes down to nanomolar concentrations that result in partial dissociation of octasomes. The ability of $Mg^{2+}$ to drive folding at the nucleosomal level is especially clear from the present observations.

The effect of $Mg^{2+}$ on mononucleosomes was documented previously [34]. Using electron microscope images of reconstituted linker histone-depleted mononucleosomes it was found that the number of wrapped DNA turns, averaged for the entire measured set, decreased from 1.60±0.17 (134±14 bp) in buffer containing 5 mM $Mg^{2+}$ to 1.52±0.18 (128±15 bp) in buffer without $Mg^{2+}$, concluding that this change represented unwrapping of ~10-bp at each end of the nucleosome. They surmised that this resulted from increasing electrostatic repulsion between the two DNA arms on $Mg^{2+}$ removal. These authors did not however observe a full range of dissociated particles as seen here and

most particularly they did not observe nucleosomal octamers with the exiting DNA strands crossing each other at right angles (Nt = 1.75), as seen here in abundance between 1 and 16 mM $Mg^{2+}$.

It can be seen from the distributions in Figs. 5 and 6 that the species with Nt = 1.5, in which the two exiting DNA duplexes emerge parallel to each other, is very rarely observed under all ionic conditions. The addition of $Mg^{2+}$ leads directly to the 'crossed linker' conformation. It follows that $Mg^{2+}$ is able to directly facilitate the orthogonal crossing of the two exiting duplexes. It is well known that divalent cations bind tightly to the DNA duplex and, for example, stabilize it against thermal melting. The simplest assumption is therefore that the $Mg^{2+}$ ions provide sufficient charge neutralization of phosphate groups to facilitate DNA compaction and permit crossing of the two duplexes as they exit the nucleosome.

The finding that $Mg^{2+}$ is able to stabilize the Nt = 1.75 'crossed linker' conformation is directly relevant to the observation that – in the absence of linker histone – the 30 nm nucleosomal fibre readily forms in the presence of divalent cations [22,23]. The linker histone globular domain has long been assumed to lie close to the dyad near where the DNA leaves the nucleosome, thereby defining their 'leaving angles' and controlling the conformation of the linker DNA in the fibre. This model has recently been substantiated by the crystal structure of a 167 bp chromatosome [35] showing a GH5 domain located directly on-axis, making contacts with the two exiting duplexes and with the central gyre. This location brings together the exiting linker DNAs, in the manner seen in the AFM images.

In the context of such a model it was unclear therefore how the fibre could form in the absence of linker histone, in particular bearing in mind that in EM visualizations of linker histone depleted nucleosomes the exiting duplexes are oriented randomly [36]. It is now apparent that with sufficient divalent cation the exit angles of the DNA are stabilized and the directionality of the linker DNA thereby defined: this could allow formation of the 30 nm fibre.

The stepwise disruption of the nucleosome in the manner found here has been observed with *in vitro* assembled arrays using micromechanical stretching experiments. For example, using a tandem array of 17 nucleosomes, forces less than 20 pN led to continuous unwrapping of 76 bp (about one superhelical turn) that was attributed to loss of both H2A/H2B dimers, while increased forces of >20pN led to cooperative loss of a further 82 bp, attributed to unwinding the central superhelical turn with loss of H3/H4 tetramers [37]. The similar stepwise disruption of a single 601-positioned nucleosome was verified to have three regions of strong interactions: the strongest at the dyad (S0 site) and the other two ~±40 bp from the dyad [38]. Our experimental data demonstrate similar DNA unwrapping with about 40 bp steps between averaged Lw values of the major observed subpopulations: 147, 106 and 72 and 39 bp, as seen in Fig. 5.

The use of such stretching techniques with chromatin samples has been reviewed by Bednar and Dimitrov [21] who noted that that nucleosome conformations are extremely sensitive to environmental conditions and studies carried out under even slightly different conditions cannot be

compared directly. Nucleosome stability was therefore explored here over an extensive range of concentrations, in particular at physiological conditions, taken to be 4-6 mM for $Ca^{2+}$and 2-4 mM for $Mg^{2+}$ in the interphase cell nucleus [39]. Fig. 7 shows that $Na^{+}$ concentrations in the range from 8 to 140 mM have no significant effect on the relative frequency with which octasomes are observed in our experiment and this does not exceed 5-10%. In contrast, divalent cations stabilize octasomes and the 'crossed linker' conformation: the effective range for half maximal frequency of octasome formation extends from 0.25 up to 64 mM with a maximum at about 4-6 mM $Mg^{2+}$. This range is similar to that intrinsic for nucleosome oligomerization and precipitation, i.e. for internucleosomal interactions [22, 23, 40-42]. Since the present data indicate that the 'crossed linker' conformation is maximized at about 4 mM $Mg^{2+}$, this suggests that it represents the basis for the inter-nucleosomal interactions that lead to formation of the 30 nm fibre.

Our principal conclusion is therefore that divalent cations generate the intra-nucleosomal crossing-over that provides the initial step towards compaction and convergence of neighboring nucleosomes in the formation of the chromatin fiber.

**ACKNOWLEDGEMENTS**

We are greatly indebted to Nanoimaging Core Facility director Yuri Lyubchenko personally and to the University of Nebraska Medical Center in which many of the AFM images and the preliminary data were obtained. IN and AT were supported by the Russian Science Foundation (project № 14-50-00068) and the Federal Agency of Scientific Organizations (Russia).

**REFERENCES**


[1] S.A. Grigoryev, C.L. Woodcock, Chromatin organization - the 30 nm fiber, Exp Cell Res, 318 (2012) 1448-1455.

[2] J.C. Hansen, Conformational dynamics of the chromatin fiber in solution: determinants, mechanisms, and functions, Annu Rev Biophys Biomol Struct, 31 (2002) 361-392.

[3] S. Pepenella, K.J. Murphy, J.J. Hayes, Intra- and inter-nucleosome interactions of the core histone tail domains in higher-order chromatin structure, Chromosoma, 123 (2014) 3-13.

[4] J. Ausio, The shades of gray of the chromatin fiber: recent literature provides new insights into the structure of chromatin, Bioessays, 37 (2015) 46-51.

[5] K. Maeshima, R. Imai, S. Tamura, T. Nozaki, Chromatin as dynamic 10-nm fibers, Chromosoma, 123 (2014) 225-237.

[6] T. Nozaki, K. Kaizu, C.G. Pack, S. Tamura, T. Tani, S. Hihara, T. Nagai, K. Takahashi, K. Maeshima, Flexible and dynamic nucleosome fiber in living mammalian cells, Nucleus, 4 (2013) 349-356.

[7] S.V. Razin, A.A. Gavrilov, Chromatin without the 30-nm fiber: constrained disorder instead of hierarchical folding, Epigenetics, 9 (2014) 653-657.

[8] K. Luger, A.W. Mader, R.K. Richmond, D.F. Sargent, T.J. Richmond, Crystal structure of the nucleosome core particle at 2.8 A resolution, Nature, 389 (1997) 251-260.

[9] S.G. Bavykin, S.I. Usachenko, A.O. Zalensky, A.D. Mirzabekov, Structure of nucleosomes and organization of internucleosomal DNA in chromatin, J Mol Biol, 212 (1990) 495-511.

[10] N. Davies, G.G. Lindsey, Histone-DNA contacts in the 167 bp 2-turn core particle, Biochim Biophys Acta, 1129 (1991) 57-63.

[11] G.G. Lindsey, P. Thompson, Isolation and characterisation of a 167 bp core particle isolated from stripped chicken erythrocyte chromatin, Biochim Biophys Acta, 1009 (1989) 257-263.

[12] K. van Holde, J. Zlatanova, The nucleosome core particle: does it have structural and physiologic relevance?, Bioessays, 21 (1999) 776-780.

[13] W.O. Weischet, J.R. Allen, G. Riedel, K.E. Van Holde, The effects of salt concentration and H-1 depletion on the digestion of calf thymus chromatin by micrococcal nuclease, Nucleic Acids Res, 6 (1979) 1843-1862.

[14] A.J. Katan, R. Vlijm, A. Lusser, C. Dekker, Dynamics of nucleosomal structures measured by high-speed atomic force microscopy, Small, 11 (2015) 976-984.

[15] K. Luger, M.L. Dechassa, D.J. Tremethick, New insights into nucleosome and chromatin structure: an ordered state or a disordered affair? Nat Rev Mol Cell Biol, 13 (2012) 436-447.

[16] H.S. Rhee, A.R. Bataille, L. Zhang, B.F. Pugh, Subnucleosomal structures and nucleosome asymmetry across a genome, Cell, 159 (2014) 1377-1388.

[17] R. Vlijm, M. Lee, J. Lipfert, A. Lusser, C. Dekker, N.H. Dekker, Nucleosome assembly dynamics involve spontaneous fluctuations in the handedness of tetrasomes, Cell Rep, 10 (2015) 216-225.

[18] J. Zlatanova, T.C. Bishop, J.M. Victor, V. Jackson, K. van Holde, The nucleosome family: dynamic and growing, Structure, 17 (2009) 160-171.

[19] A. Gansen, A. Valeri, F. Hauger, S. Felekyan, S. Kalinin, K. Tóth, J. Langowski, C. Seidel, Nucleosome disassembly intermediates characterized by single-molecule FRET. *Proc. Natl. Acad. Sci. USA*, 106, (2009) 15308–15313.

[20] Y. Katan-Khaykovich, K. Struhl, Splitting of H3–H4 tetramers at transcriptionally active genes undergoing dynamic histone exchange. *Proc. Natl. Acad. Sci. USA*, 108, (2011) 1296–1301.

[21] J. Bednar, S. Dimitrov, Chromatin under mechanical stress: from single 30 nm fibers to single nucleosomes, FEBS J, 278 (2011) 2231-2243.

[22] P.M. Schwarz, A. Felthauser, T.M. Fletcher, J.C. Hansen, Reversible oligonucleosome self-association: dependence on divalent cations and core histone tail domains, Biogchemistry, 35 (1996) 4009-4015.

[23] P.M. Schwarz, J.C. Hansen, Formation and stability of higher order chromatin structures. Contributions of the histone octamer, J Biol Chem, 269 (1994) 16284-16289.

[24] P.T. Lowary, J. Widom, New DNA sequence rules for high affinity binding to histone octamer and sequence-directed nucleosome positioning, J Mol Biol, 276 (1998) 19-42.

[25] P.N. Dyer, R.S. Edayathumangalam, C.L. White, Y. Bao, S. Chakravarthy, U.M. Muthurajan, K. Luger, Reconstitution of nucleosome core particles from recombinant histones and DNA, Methods Enzymol, 375 (2004) 23-44.

[26] Y.L. Lyubchenko, L.S. Shlyakhtenko, A.A. Gall, Atomic force microscopy imaging and probing of DNA, proteins, and protein DNA complexes: silatrane surface chemistry, Methods Mol Biol, 543 (2009) 337-351.

[27] R.M. Henderson, S. Schneider, Q. Li, D. Hornby, S.J. White, H. Oberleithner, Imaging ROMK1 inwardly rectifying ATP-sensitive K+ channel protein using atomic force microscopy, Proc Natl Acad Sci U S A, 93 (1996) 8756-8760.

[28] G. Rychkov, I. Nazarov, A. Ilatovskiy, A. Shvetsov, D. Lebedev, V. Isaev-Ivanov, A. Onufriev, Nucleosomal intermediate structures characterized by molecular dynamics simulations and atomic force microscopy, FEBS J., 281 (Suppl. 1) (2014) 707-708.

[29] G. Rychkov, I. Nazarov, A. Ilatovskiy, A. Onufriev, Partially assembled nucleosome structures at atomic detail, (in preparation).

[30] C. Claudet, D. Angelov, P. Bouvet, S. Dimitrov, J. Bednar, Histone octamer instability under single molecule experiment conditions, Journal of Biological Chemistry, 280 (2005) 19958-19965.

[31] G. Li, M. Levitus, C. Bustamante, J. Widom, Rapid spontaneous accessibility of nucleosomal DNA, Nature Structural & Molecular Biology, 12 (2005) 46-53.

[32] K.J. Polach, J. Widom, Mechanism of Protein Access to Specific DNA-Sequences in Chromatin - a Dynamic Equilibrium-Model for Gene-Regulation, Journal of Molecular Biology, 254 (1995) 130-149.

[33] B.W. Baer, D. Rhodes, Eukaryotic RNA Polymerase-II Binds to Nucleosome Cores from Transcribed Genes, Nature, 301 (1983) 482-488.

[34] A. Hamiche, P. Schultz, V. Ramakrishnan, P. Oudet, A. Prunell, Linker histone-dependent DNA structure in linear mononucleosomes, Journal of Molecular Biology, 257 (1996) 30-42.

[35] B.-R. Zhou, J. Jiang, H. Feng, R. Ghirlando, T.S. Xiao, Y. Bai, Structural Mechanisms of Nucleosome Recognition by Linker Histones, Mol. Cell, 59 (2015) 628-638.

[36] F. Thoma, T. Koller, A. Klug, Involvement of histone H1 in the organization of the nucleosome and of the salt-dependent superstructures of chromatin, J Cell Biol, 83 (1979) 403-427.

[37] B.D. Brower-Toland, C.L. Smith, R.C. Yeh, J.T. Lis, C.L. Peterson, M.D. Wang, Mechanical disruption of individual nucleosomes reveals a reversible multistage release of DNA, Proc Natl Acad Sci U S A, 99 (2002) 1960-1965.

[38] M.A. Hall, A. Shundrovsky, L. Bai, R.M. Fulbright, J.T. Lis, M.D. Wang, High-resolution dynamic mapping of histone-DNA interactions in a nucleosome, Nat Struct Mol Biol, 16 (2009) 124-129.

[39] R. Strick, P.L. Strissel, K. Gavrilov, R. Levi-Setti, Cation-chromatin binding as shown by ion microscopy is essential for the structural integrity of chromosomes, J Cell Biol, 155 (2001) 899-910.

[40] A. Bertin, S. Mangenot, M. Renouard, D. Durand, F. Livolant, Structure and phase diagram of nucleosome core particles aggregated by multivalent cations, Biophys J, 93 (2007) 3652-3663.

[41] M. de Frutos, E. Raspaud, A. Leforestier, F. Livolant, Aggregation of nucleosomes by divalent cations, Biophys J, 81 (2001) 1127-1132.

[42] B. Dorigo, T. Schalch, K. Bystricky, T.J. Richmond, Chromatin fiber folding: requirement for the histone H4 N-terminal tail, J Mol Biol, 327 (2003) 85-96.

**Figure and Table Captions**

Fig. 1. **A.** Schematic representation of DNA arm length measurement. The green circle is the histone core. Blue solid lines represent the real DNA contour. Black dashed lines represent the observed nucleosome contour in AFM images. L1, L2 are DNA arm lengths. The length of the each arm was measured from its end (at half of DNA height) up to the perpendicular line crossing the nucleosome core through its centroid. **B** is an AFM image corresponding to the nucleosome drawn in A.

Fig. 2. Nucleosome variants and their characteristics obtained from analysis of AFM images. The top row gives examples of nucleosome images corresponding to the models in the second row and their characteristics arranged in the table columns below. Curved arrows in the models indicate the total DNA bending angle (∠r) relative to unbent DNA template. Columns give corresponding values of measured angle (∠m), measured wrapped DNA length (Lw), the calculated bending angles ∠r, the calculated number of superhelical turns (Nt). Rows 3 and 4 give information for type-dependent calculations.

Fig. 3: **A:** Electrophoresis of template DNA: ethidium bromide stained 1.5 % agarose gel electrophoresis in 0.5 x TBE of the 353-bp DNA fragment (track D) containing the nucleosome-positioning sequence. **B:** ethidium bromide stained 6% polyacrylamide gel electrophoresis in 0.5 x TBE of a reconstituted nucleosome sample. The labels **d**, **n**, and **a** correspond to free DNA, the mononucleosome and a higher-molecular weight structure [25], respectively. M1 and M2 are molecular weight markers.

Fig. 4. Value distributions of wrapped nucleosome DNA length (Lw), the number of DNA superhelical turns (Nt), and the nucleosome volume in TE buffer (n = 215); in 10 mM Tris-HCl, pH 7,8 + 140 mM NaCl (n = 270) and in 10 mM Tris-HCl, pH 7,8 + 4 mM $MgCl_2$ (n = 318).

Fig. 5. Plots of wrapped nucleosome DNA length (Lw) against number of DNA superhelical turns (Nt) in TE buffer (n = 215); in 10 mM Tris-HCl, pH 7,8 + 140 mM NaCl (n = 270) and in 10 mM Tris-HCl, pH 7,8 + 4 mM $MgCl_2$ (n = 318). Left hand panels are scatter plots, right hand panels are dot density plots.

Fig. 6. Plots of nucleosome volume (V) against number of DNA superhelical turns (Nt) in TE buffer (n = 215); in 10 mM Tris-HCl, pH 7,8 + 140 mM NaCl (n = 270) and in 10 mM Tris-HCl, pH 7,8 + 4 mM $MgCl_2$ (n = 318). Left hand panels are scatter plots and the red dots represent the relative volumes, V, of octasome, hexasome, tetrasome and disome, as given in Table 1. The blue triangles represent the predicted relative volumes of particles having the same Nt values but retaining the full complement of octameric core histones. The right hand panels are dot density plots, as in Fig. 5.

Fig. 7. Relative frequencies of octasomes in 10 mM Tris-HCl, pH 7,8 with different concentrations of $MgCl_2$ (left) or NaCl (right). 1, 2, 3 – the data of three independent experiments, each of which represents the results of a separate nucleosome reconstitution and sample preparation. Each point represents the analysis of more than a hundred individual nucleosomes.

Table 1. Fractional volumes ($V_f$) of subnucleosomal particles calculated from molecular weights and normalised relative to an octasome volume of 1, experimentally measured as 180 $nm^3$.
* Mean values of Lw observed for the given subpopulation.

# Supplementary Materials

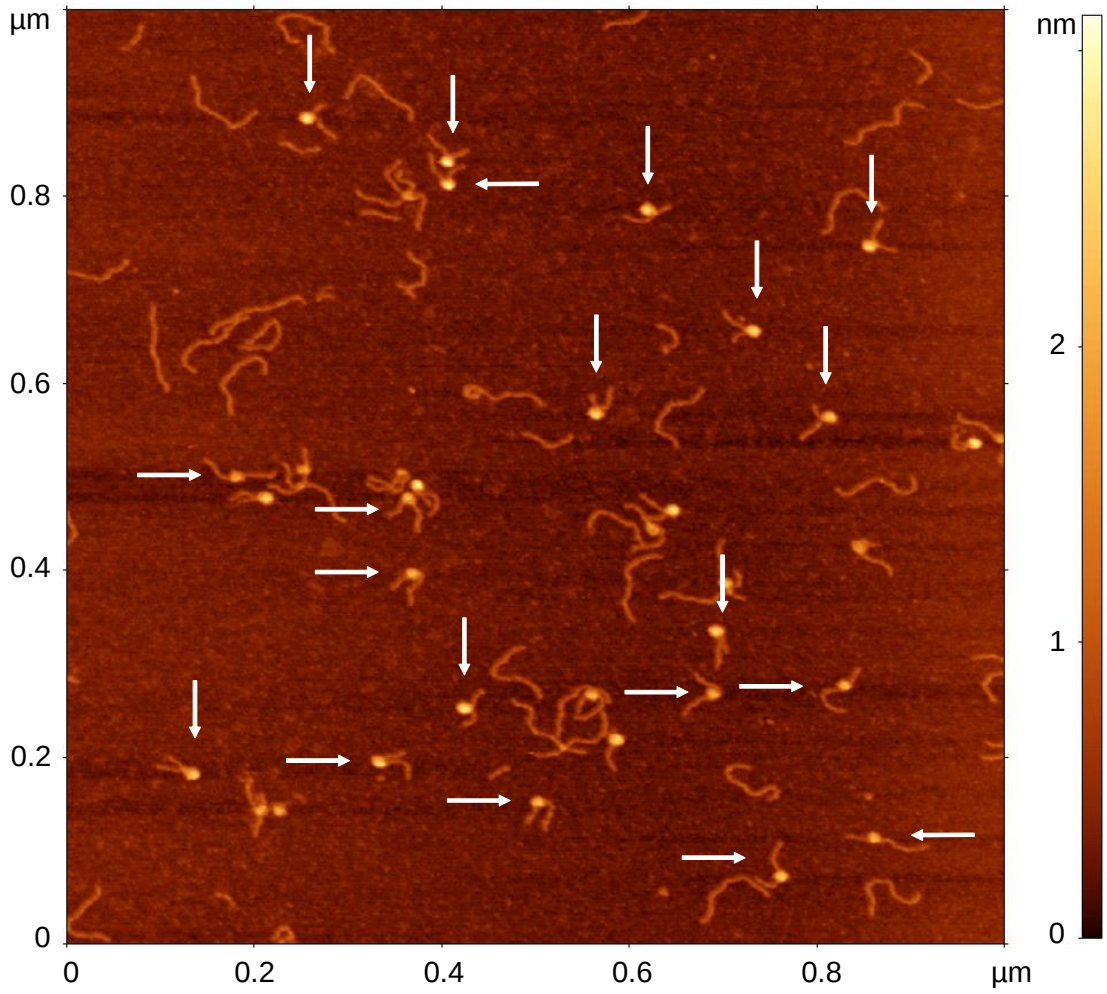


**Supplementary Fig. S1**. Typical AFM field obtained in TE plus 4 mM $Mg^{2+}$. Vertical arrows designate octasomes with Nt > 1.5 superhelical turns and Lw > 125 bp and having crossed DNA duplexes at the entry/exit point of the nucleosome. Horizontal arrows designate other nucleosome and sub-nucleosome conformations having Nt ≤ 1.5 superhelical turns and Lw ≤ 125 bp.

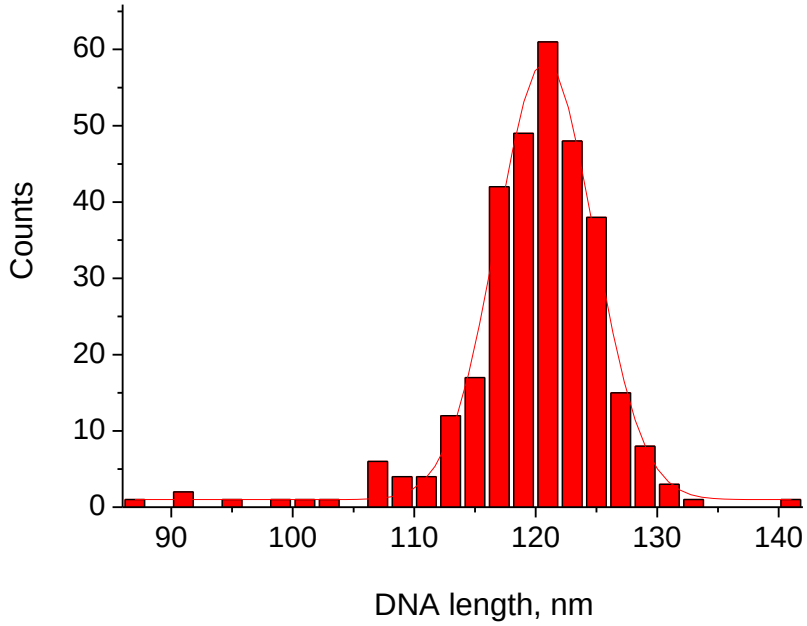


**Supplementary Fig. S2.** Distribution of free 353 bp template DNA molecules (n=316) with a Gaussian fit having a center at 120.8 ± 4.0 nm (mean ± SD). This implies a base pair repeat of 1208/353 = 3.42 A, i.e. B-form DNA.

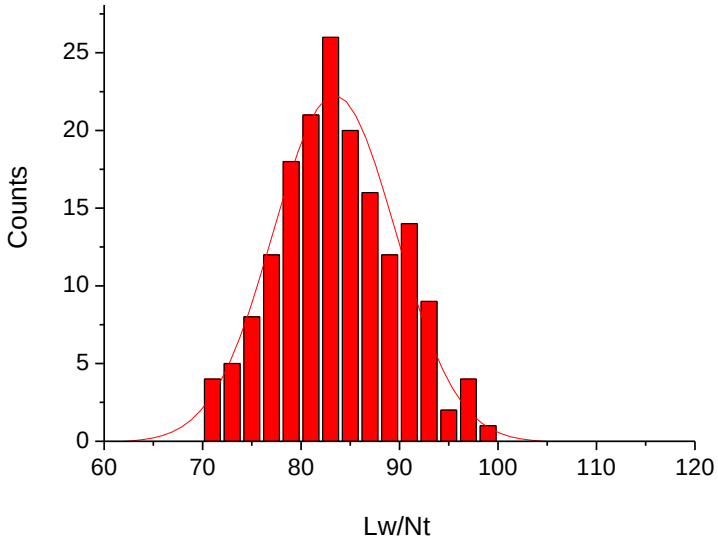


**Supplementary Fig.S3.** Distribution of Lw/Nt values for octasomes (n = 172) with a Gaussian fit centred on 83.4 ± 6.2 bp (Mean ± SD) which represents the number of base pairs per superhelical turn. The value of Nt was calculated from the angle between the two exiting DNA strands (∠m) using the equation: Nt = (540º +∠m)/360º. Lw was determined by subtracting the summed length of the two arms (L1 + L2) from the total DNA length, Lt.